Theoretical study of the gas-phase reactions of CHF_2OCHF_2 (HFE-134) with Cl atoms

Kh. Jogeshwari Devi and Asit K. Chandra*

Department of Chemistry, North-Eastern Hill University, Shillong 793 022, India

Theoretical studies have been carried out on the mechanism, kinetics and thermochemistry of the gas-phase reactions between CHF_2OCHF_2 (HFE-134) and Cl atom using the high-level *ab initio* G2(MP2) and hybrid density functional model MPWB1K methods. Two conformers relatively close in energy have been identified for CHF_2OCHF_2, both of them are likely to be important in the temperature range of our study. The hydrogen abstraction pathway for the reactions of the two lower energy conformers with the Cl atom has been studied and the rate constants determined in a wide temperature range of 250–1000 K. The G2(MP2) calculated total rate constant value of 5.9×10^{-16} cm^3 molecule^{-1} s^{-1} at 296 K is found to be in good agreement with the recent experimental value of $(5.7 \pm 1.5) \times 10^{-16}$ cm^3 molecule^{-1} s^{-1} at 296 ± 1 K. The rate constant value obtained from the MPWB1K method (8.6×10^{-17} cm^3 molecule^{-1} s^{-1}) is found to be somewhat lower than the available experimental result. The heats of formation for the CHF_2OCHF_2 molecule and the CHF_2OCF_2 radical and the atmospheric lifetime of CHF_2OCHF_2 are also reported.

Keywords: Gas-phase reactions, heat of formation, hydrogen abstraction, rate constants.

Introduction

ADVERSE environmental impact of chlorofluorocarbons (CFCs) in the atmosphere has been recognized long ago[1] and their commercial production is banned as per the Montreal Protocol[2]. Hydrochlorofluorocarbons (HCFCs) were selected as the first-generation CFC replacements because of their higher reactivity towards tropospheric oxidizing agents due to the presence of the H-atom and the resulting shorter lifetime. Later hydrofluoroethers (HFEs) have been considered as the most potential replacements for CFCs and HCFCs, because they are chlorine-free compounds and the presence of ether linkage (–O–) generally increases their reactivity and reduces atmospheric lifetime. Thus HFEs are found to be a better alternative in industrial applications such as heat-transfer fluid in refrigeration systems, cleaning agent in electronic industry, foam-blowing and also for lubricant deposition[3–5]. Although HFEs do not contain Cl atom and thus their stratospheric ozone depletion potential is zero, they have strong absorption in the 1000–3000 cm^{-1} range and are potential greenhouse gases[6,7]. The atmospheric chemistry of HFEs is therefore important to assess their harmful effects on atmosphere. The reaction with OH radical is known to be the main channel of degradation for organic species in atmosphere[8–10], and primarily decides its atmospheric lifetime. But the gas-phase reactions of Cl atoms with organic compounds are also known to be an important loss process of organic compounds in atmosphere, especially in the coastal atmosphere because of higher concentration of Cl atoms[11,12]. Moreover, in many cases the reactivity of Cl atoms toward organic compounds is found to be higher than that for OH radicals[13,14]. Because of this importance, there are many recent experimental and theoretical studies on the reactions of HFEs with Cl atoms[15–20]. In fact, development of theoretical procedures and availability of powerful computers make it possible (necessary as well) now-a-days to gain additional support for experimental kinetics results from theoretical studies. The global warming potential (GWP) of CHF_2OCHF_2 has also been recently reported: they are 8448 and 3617 in 20 and 100 years time horizon respectively[21].

In the present work, we have studied the hydrogen abstraction reactions between CHF_2OCHF_2 and Cl atom using quantum chemical methods. To the best of our knowledge, this is the first detailed theoretical study for this important reaction. The reaction was first studied experimentally using very low pressure reactor (VLPR) method by Kambanis *et al.*[22]. They reported the absolute rate constants in the temperature range 273–363 K by the expression (in cm^3 molecule^{-1} s^{-1}): $(1.03 \pm 0.19) \times 10^{-12}$ exp(–867 ± 106/*T*), which gives a rate constant (*k*) value of 5.6×10^{-14} cm^3 molecule^{-1} s^{-1} at 298 K. This value is more than an order of magnitude larger than the established rate constant value of 2.4×10^{-15} cm^3 molecule^{-1} s^{-1} at 298 K for the reaction between CHF_2OCHF_2 and OH radical[23]. Surprisingly, the rate constant values for the reactions of $CF_3CHClOCHF_2$ and $CHF_2OCF_2OCHF_2$ with Cl atoms are 10 to 1000 times smaller[24,25] than the value reported by Kambanis *et al.*[22] for CHF_2OCHF_2+Cl reactions, although they are likely to have similar reactivity. Recently, Andersen *et al.*[26] performed another experimental study using smog chamber/FTIR techniques on the

*For correspondence. (e-mail: akchandra@nehu.ac.in)

title reaction for better understanding and to find out any error in the previously reported kinetic data. Interestingly, they reported a rate constant value of $(5.7 \pm 1.5) \times 10^{-16}$ cm^3 molecule^{-1} s^{-1} at 296 ± 1 K, which is 100 times lower than the value reported by Kambanis *et al.*[22]. Since the experimental study provides mainly the total rate constant, the mechanism and thermochemistry of this reaction are not yet known. Moreover, because of these two conflicting experimental results, we feel it is necessary to have detailed theoretical studies of the titled reaction to resolve it. Hence we set out to study the reaction (R1) using *ab initio* G2(MP2) and DFT-based MPWB1K quantum chemical methods and kinetic modelling for the better understanding of this reaction as well as to remove the ambiguity originating from the two conflicting experimental results.

$$CHF_2OCHF_2 + Cl \rightarrow CHF_2OCF_2 + HCl. \quad \text{(R1)}$$

We present here the potential energy profile (including geometries, energies and vibrational frequencies of reactants, transition states, products) and kinetic data for this reaction along with the relative importance for each reaction channel. We also report here the rate constant for the reaction in a wide temperature range of 250–1000 K.

Computational method

The geometries of reactant (CHF_2OCHF_2), transition states (TS) for hydrogen abstraction reactions and radicals produced after hydrogen abstraction from CHF_2OCHF_2 were optimized using the MPWB1K/6-31+G(d,p) method[27]. The MPWB1K method is specifically developed for kinetic modelling and is known to produce reliable results[28–30].

Frequency calculations were performed at each stationary point to characterize the minimum energy equilibrium structure (having all real frequencies) and transition state (with one imaginary frequency). Normal mode analysis of TS also confirms that the imaginary frequency in TS corresponds to the coupling of stretching modes of the breaking C–H and forming H–Cl bonds. Finally high-level *ab initio* G2(MP2) calculations were performed for all the stationary points along the potential energy surface of the reaction at the MPWB1K optimized structure for further refinement of our results. The zero point energy (ZPE) obtained at the MPWB1K level was used while estimating the G2(MP2) energy[31]. This dual level calculation (G2(MP2)/MPWB1K) is known to produce reliable kinetic data[32]. All electronic structure calculations were performed by using the Gaussion-03 suite of programs[33]. The rate constant for hydrogen abstraction reaction was estimated using the conventional transition state theory (TST) equation[34]:

$$k(T) = \sigma_r \Gamma(T) \frac{k_B T}{h} \frac{q_{TS}(T)}{q_{HFE}(T) \cdot q_{Cl}(T)} e^{-\Delta E_0^{\#}/RT}, \quad (1)$$

where $q_x(T)$ represents the partition function for the species x (TS, HFE and Cl) at temperature T, k_B is the Boltzmann constant, $\Delta E_0^{\#}$ is the barrier height and σ_r is the degeneracy of each reaction channel. $\Gamma(T)$ is the tunnelling correction factor for taking care of tunnelling contribution in H-abstraction reaction and it is simply interpreted as the ratio of quantum mechanical rate over classical mechanical rate[35]. Tunnelling is a quantum mechanical phenomenon and plays an important role for H-atom transfer reactions. The tunnelling correction $\Gamma(T)$ was estimated by using the Eckart's unsymmetric barrier method[35]. In this method, the reaction path through TS is fitted first in a model potential function

$$V(y) = \frac{Ay}{1-y} - \frac{By}{(1-y)^2}, \quad (2)$$

where $y = -\exp(2\pi x/L)$, and x is the displacement along the reaction coordinate and L is a characteristic length[35]. The A and B are two parameters that depend upon forward and reverse barrier heights. $\Gamma(T)$ was estimated by numerically integrating the tunnelling probability, $\alpha(E)$, for this potential function over all possible values of energy and divided by the classical probability[36],

$$\Gamma(T) = e^{\Delta E^{\#}/k_B T} \int_0^{\infty} e^{-E/k_B T} \alpha(E) d(E/k_B T). \quad (3)$$

The values of $\Gamma(T)$ vary in the range 3.8 at 250 K to almost 1.0 at 1000 K for different reaction channels of (R1).

Partition functions were calculated using rigid rotor and harmonic oscillator (HO) model. It should be mentioned that several authors have pointed out the importance of treating low frequency torsional motion as hindered rotor and the corresponding HO partition function needs to be replaced by hindered rotor partition function[37,38]. However, in the present case the low frequency torsional motion is related to the rotation of the $-CHF_2$ group about the O–C bond axis. Hindered rotor corrections for such modes in CHF_2OCHF_2 and TS are likely to cancel each other and may not have any significant effect on the calculated rate constant value. For example, our calculation shows that the rate constant for the most important channel ($RC2_{SC1}$, discussed later) changes by only a factor of 1.02 at 298 K, if hindered rotor correction is made for low frequency torsion of the $-CHF_2$ group using Truhlar's method[37]. The barrier height ($\Delta E_0^{\#}$) was estimated from the energy difference, including ZPE between TS and the reactants. The electronic partition function for Cl atom was calculated considering the splitting of 881 cm^{-1} between the ground $^2P_{3/2}$ and excited $^2P_{1/2}$ electronic states of Cl atom due to spin-orbit coupling[39].

Results and discussion

Structure and energetics

Two possible conformers are found for CHF_2OCHF_2 molecule during geometry optimization. Structures of these conformers (SC1 and SC2) are shown in Figure 1. SC1 is the most stable conformer of CHF_2OCHF_2 and SC2 is seen to be relatively close in energy (~1 kcal/mol). The two H-atoms in SC1 are stereographically non-equivalent, whereas SC2 has a C2 symmetry and both the H-atoms are equivalent. Since these two conformers of CHF_2OCHF_2 are closer in energy, both of them need to be considered while studying reaction R1.

We could find one TS each for hydrogen abstraction by Cl atom from the C2–H4 ($TS1_{SC1}$) and C3–H7 ($TS2_{SC1}$) bond of the SC1 conformer of CHF_2OCHF_2. These two reaction channels originating from the SC1 conformer of CHF_2OCHF_2 are henceforth designated as $R1_{SC1}$. On the other hand, only one TS (TS_{SC2}) was found for hydrogen abstraction from the SC2 conformer of CHF_2OCHF_2, since both the H-atoms are equivalent, and this channel is marked as $R1_{SC2}$. A schematic diagram of the reaction R1 is shown in Figure 2. The MPWB1K optimized structures for all these TS, HCl and product radicals are also given in Figure 1 along with some key geometrical parameters; whereas the detailed structures are given in Table 1. The breaking C–H bond and the forming H…Cl bond in TS structures are found to be 31% and 12% longer than the C–H bond length in isolated CHF_2OCHF_2 and in HCl respectively. It shows that the barrier of this reaction (R1) lies near the products, indicating that the reaction with Cl atoms proceeds through formation of a late TS. The product-like structure of TS also becomes obvious if one compares the structure of TS and CHF_2OCF_2 radical. This is of course expected for an endothermic reaction in view of Hammond's postulate[40]. The vibrational frequencies for all the stationary points involved in reaction R1 are given in Table 2 along with the rotational constants. These data can be useful for further thermo-kinetic modelling of other reactions involving these species. The $\langle S^2 \rangle$ expectation values given in Table 2 show that the

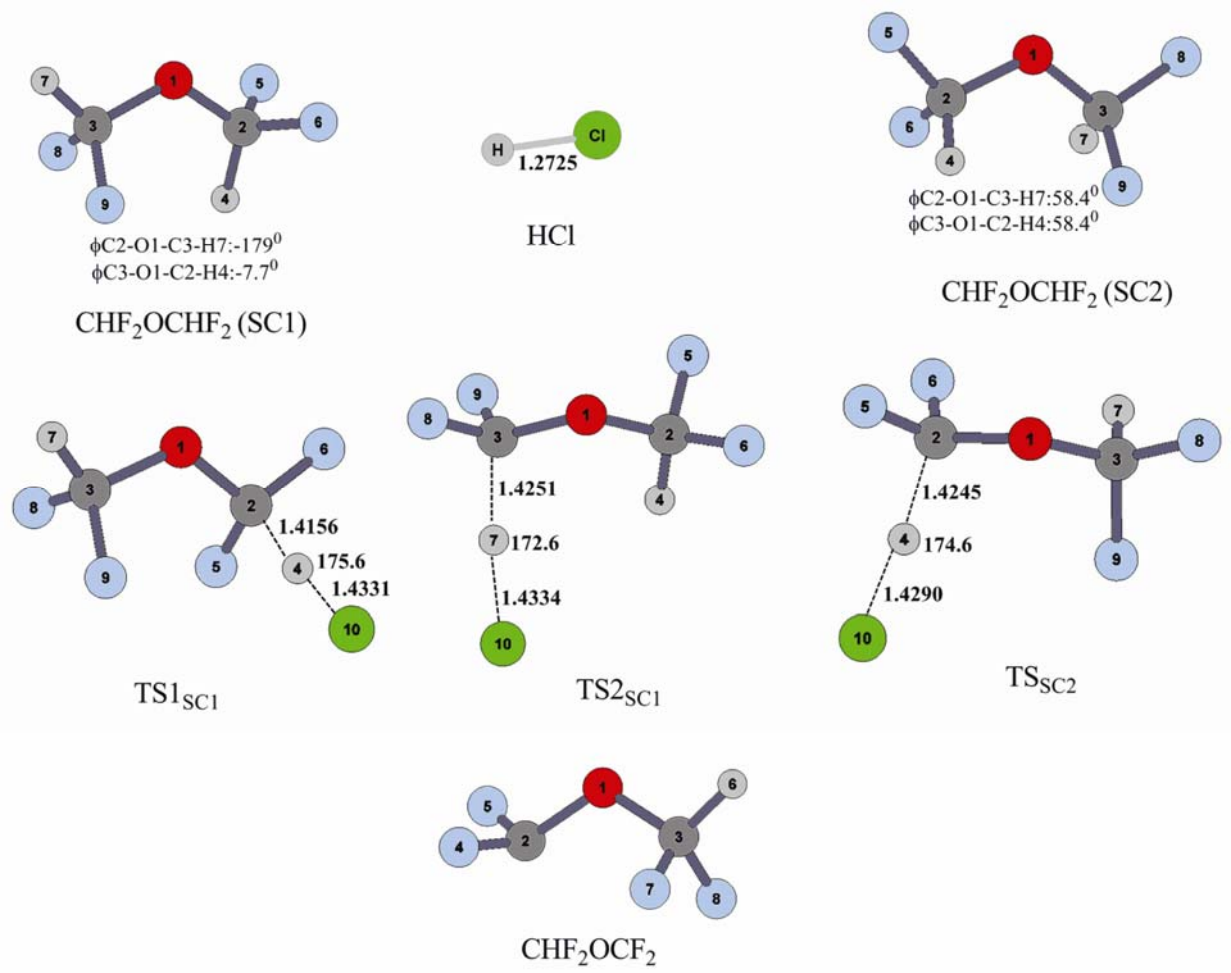

Figure 1. MPWB1K/6-31+G(d,p) optimized structures of the two conformers of CHF_2OCHF_2, CHF_2OCF_2 radical, HCl and transition states for hydrogen abstraction by Cl atoms from the SC1 and SC2 conformers of CHF_2OCHF_2. Bond lengths and angles are given in Å and degrees respectively.

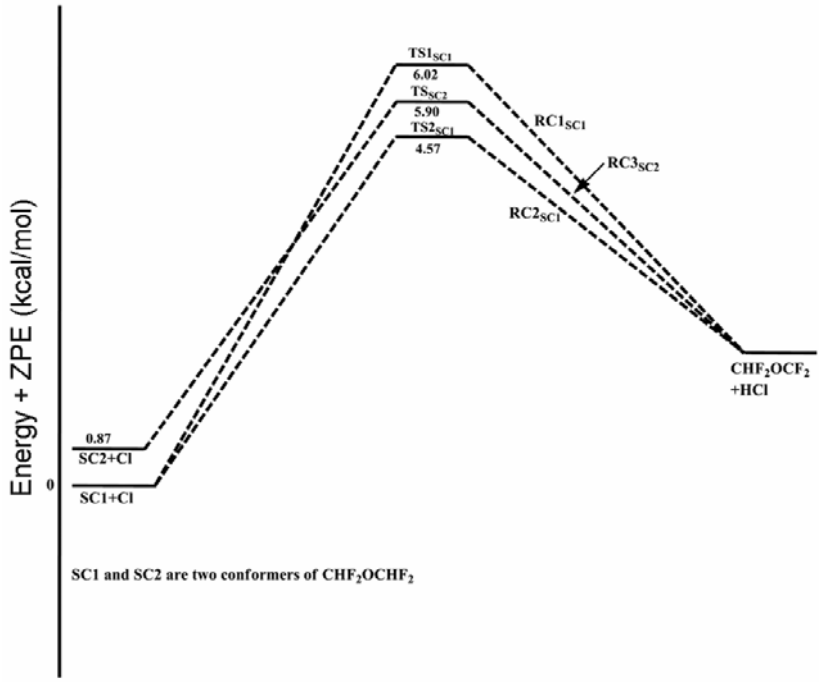

Figure 2. Schematic diagram of the potential energy profile for the reaction between CHF_2OCHF_2 and Cl atom.

Table 1. MPWB1K optimized geometrical parameters of the two conformers of CHF_2OCHF_2 molecule (SC1 and SC2), transition states for hydrogen abstraction by Cl atom from SC1 ($TS1_{SC1}$ and $TS2_{SC1}$) and SC2 (TS_{SC2}) and CHF_2OCF_2 radical. Bond lengths and angles are given in Å and degrees respectively. See Figure 1 for atom numbering

Parameter	SC1	SC2	$TS1_{SC1}$	$TS2_{SC1}$	TS_{SC2}	CHF_2OCF_2
O1-C2	1.3720	1.3463	1.3409	1.3876	1.3331	1.3485
O1-C3	1.3531	1.3463	1.3784	1.3306	1.3862	1.3656
C2-H4	1.0849	1.0857	1.4156	1.0864	1.4245	
C2-F5/F4	1.3337	1.3236	1.3140	1.3298	1.3036	1.3159
C2-F6/F5	1.3316	1.3469	1.3058	1.3205	1.3242	1.3093
C3-H7H6	1.0816	1.0857	1.0820	1.4251	1.0848	1.0821
C3-F8/F7	1.3428	1.3236	1.3304	1.3032	1.3199	1.3356
C3-F9/F8	1.3442	1.3469	1.3308	1.3185	1.3297	1.3358
C2O1C3	116.6	115.8	118.8	117.7	117.7	116.9

spin contamination effect is negligible for the open-shell species (TS and radical) involved in our study, justifying our single configuration calculations.

The relative energies (including ZPE) for all the species involved in reactions R1 are given in Table 3, whereas the same is also indicated in a schematic diagram of the potential energy surface as shown in Figure 2. The energy difference between the two conformers of CHF_2OCHF_2 is calculated to be 0.87 and 1.12 kcal/mol at the G2(MP2) and MPWB1K level respectively. This small energy difference between SC1 and SC2 implies that population of SC2 will be about 19% at 298 K and almost 40% at 1000 K. Hence hydrogen abstraction from both the conformers needs to be considered while estimating the total rate constant for reaction R1. The G2(MP2) calculated barrier heights ($TS1_{SC1}$ and $TS2_{SC1}$) for hydrogen abstraction from the SC1 conformer of CHF_2OCHF_2 are 6.02 and 4.57 kcal/mol respectively, whereas these values are 6.80 and 5.92 kcal/mol at the MPWB1K level. On the other hand, the barrier height (TS_{SC2}) for hydrogen abstraction from the SC2 conformer of CHF_2OCHF_2 is 5.03 and 5.95 kcal/mol at the G2(MP2) and MPWB1K level respectively. The barrier heights obtained from the MPWB1K results are 0.8 to 1.3 kcal/mol higher than that obtained at the G2(MP2) level.

The enthalpy of reaction ($\Delta_r H^0_{298}$) values tabulated in Table 3 for $RC1_{SC1}$ and $RC3_{SC2}$ show that both the reactions are slightly endothermic in nature at 298 K. Our G2(MP2)-calculated $\Delta_r H^0_{298}$ values amount to 2.10 and 1.36 kcal/mol for $RC1_{SC1}$ (also $RC2_{SC1}$) and $RC3_{SC2}$ respectively. The $\Delta_r H^0_{298}$ values obtained from the G2(MP2) and MPWB1K methods for $RC1_{SC1}$ at 298 K differ by

Table 2. Harmonic vibrational frequencies (cm^{-1}) and rotational constants (GHz, within bracket) calculated at the MPWB1K/6-31+G(d,p) level

System	Frequency (cm^{-1})	$\langle S^2 \rangle$[a]
CHF_2OCHF_2 (SC1)	17, 81, 199, 409, 469, 541, 600, 648, 816, 1072, 1157, 1204, 1214, 1227, 1291, 1407, 1417, 1448, 1488, 3233, 3277 [4.68572, 1.94347, 1.54572]	0
CHF_2OCHF_2 (SC2)	55, 106, 186, 374, 483, 545, 601, 638, 795, 1128, 1146, 1201, 1222, 1264, 1280, 1412, 1443, 1450, 1491, 3226, 3228 [5.32430, 1.59785, 1.49942]	0
$TS1_{SC1}$	*947i*, 48, 63, 116, 151, 212, 324, 389, 512, 538, 570, 766, 830, 963, 1014, 1093, 1180, 1210, 1232, 1314, 1376, 1424, 1469, 3273 [2.11192, 1.14544, 0.87881]	0.7584 (0.7836)
$TS2_{SC1}$	*823i*, 40, 82, 110, 121, 227, 352, 387, 420, 558, 633, 680, 817, 976, 1048, 1136, 1174, 1209, 1250, 1341, 1396, 1436, 1481, 3221 [1.78191, 1.07874, 0.84540]	0.7580 (0.7820)
TS_{SC2}	*949i*, 23, 60, 113, 144, 198, 327, 382, 492, 556, 611, 667, 847, 975, 1081, 1132, 1196, 1199, 1257, 1318, 1388, 1443, 1466, 3240 [1.96528, 1.07760, 0.80764]	0.7584 (0.7836)
CHF_2OCF_2	45, 92, 194, 403, 470, 541, 596, 661, 819, 1044, 1191, 1199, 1253, 1294, 1345, 1418, 1466, 3269 [4.79940, 1.97934, 1.57605]	0.7520 (0.7542)
HCl	3084 [318.60504]	0

[a]Values within parenthesis correspond to the $\langle S^2 \rangle$ values at the HF/6-311G** level.

Table 3. Relative energies (ΔE_{rel} in kcal/mol, including ZPE) for all species involved in reaction channels ($RC1_{SC1}$, $RC2_{SC1}$ and $RC3_{SC2}$) of CHF_2OCHF_2 reactions with Cl atom. Reaction enthalpy ($\Delta_rH^0_{298}$), free energy ($\Delta_rG^0_{298}$) and bond dissociation enthalpy (D^0_{298}) at 298 K as obtained at the G2(MP2) and MPWB1K level. Data are in kcal/mol

	G2 (MP2)	MPWB1K
ΔE_{rel}		
CHF_2OCHF_2 (SC1)	0	0
CHF_2OCHF_2 (SC2)	0.87	1.12
$TS1_{SC1}$	6.02	6.80
$TS2_{SC1}$	4.57	5.92
TS_{SC2}	5.90	7.07
$\Delta_rH^0_{298}$		
$RC1_{SC1}/RC2_{SC1}$	2.10	3.25
$RC3_{SC2}$	1.36	2.18
$\Delta_rG^0_{298}$		
$RC1_{SC1}/RC2_{SC1}$	0.40	1.55
$RC3_{SC2}$	–1.16	–0.69
D^0_{298}		
$CHF_2OCHF_2 \rightarrow CHF_2OCF_2 + H$	106.1 (104.0 ± 1.0)[a]	101.6
$HCl \rightarrow Cl + H$	104.0 (103.1)[a]	98.3

[a]Experimental value from Lide[41].

1.1 kcal/mol, whereas the same for $RC3_{SC2}$ differ by only 1.2 kcal/mol. This small difference suggests that the MPWB1K method provides thermochemical data which are comparable to the much more expensive G2(MP2) method.

The bond dissociation enthalpy value D^0_{298}, value obtained from the G2(MP2) results for the C–H bond in the SC1 and SC2 conformers of CHF_2OCHF_2 molecule is listed in Table 3. Our G2(MP2)-calculated D^0_{298} values for the C–H bond in SC1 and SC2 conformers are 106.1 and 105.4 kcal/mol respectively, which is in reasonably good agreement with the experimental value[41] of 104.0 ± 1.0 kcal/mol and other values of 103.9 and 103.4 kcal/mol from the literature[15,42]. Moreover, our G2(MP2) calculated D^0_{298} value for the H–Cl bond (104.0 kcal/mol) is in excellent agreement with the experimental value of 103.1 kcal/mol. The D^0_{298} values obtained from the MPWB1K results are seen to be somewhat lower than the corresponding experimental values.

The standard enthalpy of formation ($\Delta_fH^0_{298}$) at 298 K for CHF_2OCHF_2 and the radical generated from hydrogen abstraction, CHF_2OCF_2, can be valuable information for understanding the kinetics, mechanism and thermochemical properties of their reactions and most importantly for atmospheric modelling, but these values are not yet reported. We have thus calculated the $\Delta_fH^0_{298}$ value for CHF_2OCHF_2 from the enthalpies of reaction ($\Delta_rH^0_{298}$) for the following two isodesmic reactions:

$$CHF_2OCHF_2 + 2CH_4 \rightarrow 2CH_2F_2 + CH_3OCH_3, \quad \text{(R2)}$$

$$CHF_2OCHF_2 + 2CH_4 + H_2O \rightarrow 2CH_2F_2 + 2CH_3OH. \quad \text{(R3)}$$

Since the $\Delta_rH^0_{298}$ value corresponds to the difference of the $\Delta_fH^0_{298}$ values between the products and the reactants, the $\Delta_fH^0_{298}$ value for CHF_2OCHF_2 can easily be calculated if the $\Delta_fH^0_{298}$ values for the other species in reactions R2 and R3 are known. The standard $\Delta_fH^0_{298}$ values for CH_4, H_2O, CH_2F_2, CH_3OH and CH_3OCH_3 are known to be –17.8,

Table 4. Standard enthalpy of formation ($\Delta_f H^0_{298}$) at 298 K calculated from the isodesmic reactions (R2 and R3). Data are in kcal/mol

	Reaction	G2 (MP2)	MPWB1K
CHF_2OCHF_2 (SC1)	R2	–259.8	–259.5
	R3	–259.6	–258.7
Average		(–259.7)	(–259.1)
CHF_2OCF_2		–206.6	–204.8

–57.8, –108.1, –48.0 and –44.0 kcal/mol respectively[41]. We have first calculated the $\Delta_r H^0_{298}$ values for the reactions R2 and R3 using both MPWB1K and G2(MP2) methods, and then $\Delta_f H^0_{298}$ value for CHF_2OCHF_2 was estimated using $\Delta_f H^0_{298}$ values for the other species involved in reactions R2 and R3. The $\Delta_r H^0_{298}$ values for R2 and R3 are 35.32 and 40.84 kcal/mol at the G2(MP2) level, whereas the same amount to 35.02 and 39.70 kcal/mol respectively, at the MPWB1K level. Our calculated $\Delta_f H^0_{298}$ values are listed in Table 4. The average $\Delta_f H^0_{298}$ values obtained from our calculations for the SC1 conformer of CHF_2OCHF_2 are –259.7 and –259.1 kcal/mol at the G2(MP2) and MPWB1K level respectively. The $\Delta_f H^0_{298}$ values for the CHF_2OCF_2 radical can then be easily calculated from the reported $\Delta_r H^0_{298}$ values for reaction R1 in Table 3, and the calculated $\Delta_f H^0_{298}$ value for CHF_2OCHF_2. The $\Delta_f H^0_{298}$ values for the CHF_2OCF_2 radical calculated from our G2(MP2) results are –206.6 kcal/mol.

Rate constant calculations

The rate constant for each reaction channel of reaction R1 has been estimated, as discussed before, using the TST expression (eq. (1)) and Eckart's unsymmetric barrier method for tunnelling correction in the temperature range 250–1000 K. As discussed before and shown in Figure 2, the reaction between the SC1 conformer of CHF_2OCHF_2 and Cl atoms ($R1_{SC1}$) goes through two different channels ($RC1_{SC1}$ and $RC2_{SC1}$ passing through $TS1_{SC1}$ and $TS2_{SC2}$) and therefore the rate constant for SC1 is estimated as the sum of the rate constants for these two channels ($k1_{SC1}$ and $k2_{SC1}$). On the other hand, the reaction between the SC2 conformer of CHF_2OCHF_2 and Cl atoms ($RC3_{SC2}$) has only one reaction channel. The σ_r value in eq. (1) is taken as 2 for this reaction channel due to the presence of two equivalent H-atoms. The rate constant values calculated from the G2(MP2) barrier heights for the two reaction channels originating from SC1 ($k_{SC1} = k1_{SC1} + k2_{SC1}$) and the same for SC2 ($k_{SC2}$) are listed in Table 5.

The total rate constant (k) at any temperature T is then estimated from the weighted average of the rate constant values for k_{SC1} and k_{SC2} as:

$$k(T) = w_{SC1}(T)[k1_{SC1}(T) + k2_{SC1}(T)] + w_{SC2}(T) \cdot k_{SC2}(T). \quad (4)$$

Table 5. Rate constant values (cm^3 $molecule^{-1}$ s^{-1}) for hydrogen abstraction reactions of SC1 ($k_{SC1} = k1_{SC1} + k2_{SC1}$) and SC2 ($k_{SC2}$) conformers of CHF_2OCHF_2 with Cl atoms and total rate constant values (k) for reaction (R1) using G2(MP2) barrier height

T (K)	$k_{SC1} \times 10^{15}$	$k_{SC2} \times 10^{14}$	$k \times 10^{14}$
250	0.043	0.057	0.012
298	0.182	0.253	0.061
350	0.612	0.889	0.244
450	3.38	5.20	1.67
550	11.4	18.2	6.43
650	28.9	47.1	17.8
750	60.5	100.0	39.6
850	111.0	185.1	76.2
950	185.0	311.0	132.0
1000	233.1	392.0	168.1

w_{SC1} and w_{SC2} are the temperature-dependent weight factors estimated from the Boltzmann population distribution law[43]. The calculated total rate constant (k) values for hydrogen abstraction reactions of CHF_2OCHF_2 and Cl atoms within a range 250–1000 K are given in Table 5. The rate constant values for the SC1 and SC2 conformers and the total rate constant value are also shown in Figure 3. Our calculated k value from the G2(MP2) barrier heights amount to 5.9×10^{-16} cm^3 $molecule^{-1}$ s^{-1} at 296 K, which is in excellent agreement with the most recent experimental result of $(5.7 \pm 1.5) \times 10^{-16}$ cm^3 $molecule^{-1}$ s^{-1} (ref. 26). The k value obtained from the MPWB1K results at 296 K is 8.6×10^{-17} cm^3 $molecule^{-1}$ s^{-1} and is somewhat lower than the G2(MP2) value, obviously because of larger barrier height obtained from the MPWB1K results.

Interestingly, our calculated rate constant is almost two orders of magnitude lower than that reported by Kambanis *et al.*[22]. However, we believe that our theoretically estimated rate constant value is accurate since the calculated rate constant value is comparable with that for the reaction of compound ($CHF_2OCF_2OCHF_2$) of similar reactivity with Cl atoms[25]. Our calculated rate constant value for the reaction of CHF_2OCHF_2 with Cl atom at 298 K is 6.1×10^{-16} cm^3 $molecule^{-1}$ s^{-1} and this is an order of magnitude smaller than the reported rate constant value of 2.4×10^{-15} cm^3 $molecule^{-1}$ s^{-1} for the reaction of CHF_2OCHF_2 with OH radicals[23]. It can be seen from Table 5 that the rates of hydrogen abstraction from the SC2 conformer of CHF_2OCHF_2 are faster than those from the SC1 conformer. However, the contribution of the SC1 conformer to the total rate constant (k) is higher, especially at lower temperature, because of its lower energy than the SC2 conformer and the resulting greater weight factor in eq. (4).

The Arrhenius plot of the total rate constant k exhibits significant nonlinear behaviour, mainly due to significant tunnelling contribution at lower temperature range and because of contribution from different reaction channels, which makes the pre-exponential factor highly temperature-dependent. As a general practice, hydrogen abstraction

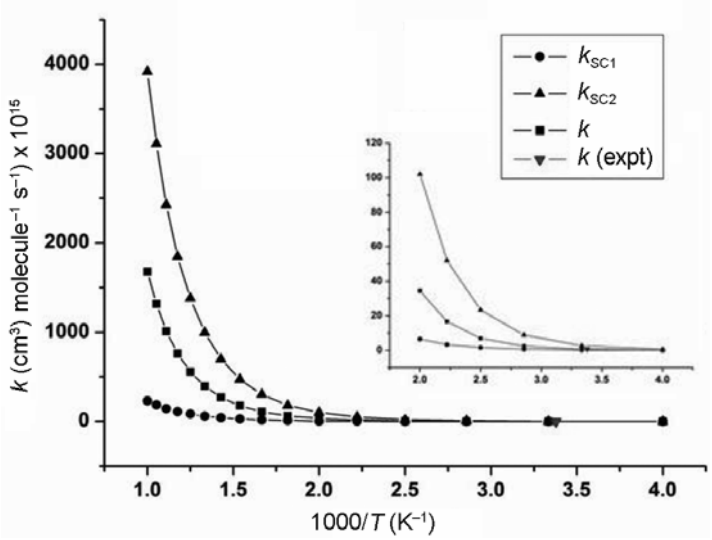

Figure 3. Rate constant for hydrogen abstraction reactions of two conformers (SC1 and SC2) of CHF_2OCHF_2 with Cl atom. (Inset) The same between 250 and 500 K. Experimental value is from Andersen *et al.*[26].

rate constant is generally expressed by a three-parameter model equation:

$$k(T) = AT^n \exp(-\Delta E^0/RT), \quad (5)$$

where A, n and ΔE^0 are the adjustable parameters. The ΔE^0 can be taken as a hypothetical reaction barrier at 0 K and is related to the activation energy as,

$$E_a = \Delta E^0 + nRT. \quad (6)$$

The calculated rate constant in the temperature range 250–1000 K can be best described by the following model equation:

$$k = 5.47 \times 10^{-21}\, T^{3.08} \exp(-1770/T). \quad (7)$$

The activation energy, E_a, estimated from eq. (6) at 298 K amounts to 5.3 kcal/mol.

Generally, the tropospheric lifetime (τ_{eff}) of CHF_2OCHF_2 can be estimated by assuming that its removal from the atmosphere occurs only through reaction with OH radicals and Cl atoms. Then τ_{eff} can be expressed as[15],

$$1/\tau_{eff} = 1/\tau_{OH} + 1/\tau_{Cl}, \quad (8)$$

where $\tau_{OH} = (k_{OH} \times [OH])^{-1}$ and $\tau_{Cl} = (k_{Cl} \times [Cl])^{-1}$. Using the 298 K value of $k_{OH} = 2.4 \times 10^{-15}$ cm^3 molecule^{-1} s^{-1} and $k_{Cl} = 6.1 \times 10^{-16}$ cm^3 molecule^{-1} s^{-1}, and the global average atmospheric OH and Cl concentration of 8.8×10^5 and 1.0×10^4 molecule/cm^3 respectively[44,45], the atmospheric lifetime for CHF_2OCHF_2 is estimated to be around 15 years. Of course, with the average global concentration of Cl atom, the contribution of Cl reaction for removal of CHF_2OCHF_2 from the atmosphere appears negligible because of larger k_{OH} value and greater OH particle density. But in coastal area the scenario may change because of much higher Cl atom concentration. Our calculated lifetime for CHF_2OCHF_2 is much longer than the value (~10 years) estimated earlier[15] using $k_{Cl} = 5.7 \times 10^{-14}$ cm^3 molecule^{-1} s^{-1}. However, it supports the most recent experimental result[26].

Conclusion

Theoretical studies have been carried out for the hydrogen abstraction reactions between CHF_2OCHF_2 and Cl atoms using *ab initio* G2(MP2) and DFT-based MPWB1K method. The G2(MP2) results are seen to be more reliable as they agree well with the most recent experimental data than the MPWB1K results. Our calculated total rate constant value $k = 5.9 \times 10^{-16}$ cm^3 molecule^{-1} s^{-1} at the G2(MP2) level supports the recently reported experimental result. We report the rate constant values for CHF_2OCHF_2 + Cl reaction in a wide temperature range of 250–1000 K. To this end, a three-parameter model equation $k = 5.47 \times 10^{-21}\, T^{3.08} \exp(-1770/T)$ has been proposed to describe rate constants in this temperature range. The $\Delta_f H^0_{298}$ values for CHF_2OCHF_2 molecule and CHF_2OCF_2 radical are predicted to be –259.7 and –206.6 kcal/mol respectively. Atmospheric lifetime of CHF_2OCHF_2 is estimated to be around 15 years.

1. Farman, J. D., Gardiner, B. G. and Shanklin, J. D., Large losses of total ozone in Antarctica reveal seasonal ClO_x/NO_x. *Nature*, 1985, **315**, 207–209.
2. World Meteorological Organization, *Scientific Assessment of Ozone Depletion, 1994*, Report No. 37, WMO, Geneva, 1995.
3. Sekiya, A. and Misaki, S., A continuing search for new refrigerants. *CHEMTECH*, 1996, **26**, 44–48.
4. Wallington, T. J., Guschin, A., Stein, J. N. N., Platz, J., Sehested, J., Christensen, L. K. and Nielsen, O. J., Atmospheric chemistry of $CF_3CH_2OCH_2CF_3$: UV spectra and kinetic data for $CF_3CH(\bullet)OCH_2CF_3$ and $CF_3CH(OO\bullet)OCH_2CF_3$ radicals and atmospheric fate of $CF_3CH(O\bullet)OCH_2CF_3$ radicals. *J. Phys. Chem. A*, 1998, **102**, 1152–1161.
5. Sekiya, A. and Misaki, S., The potential of hydrofluoroethers to replace CFCs, HCFCs and PFCs. *J. Fluorine Chem.*, 2000, **101**, 215–221.

6. Imasu, R., Suga, A. and Matsuno, T., Radiative effects and halocarbon global warming potentials of replacement compounds for chlorofluorocarbons. *J. Meteorol. Soc. Jpn.*, 1995, **73**, 1123–1136.
7. Houghton, J. T. *et al.*, *Climate Change 2001: The Scientific Basis, Contribution of Working Group I to the Third Assessment Report of the Intergovernmental Panel on Climate Change*, IPCC, Geneva, 2001.
8. Good, D. A. and Francisco, J. S., Atmospheric chemistry of alternative fuels and alternative chlorofluorocarbons. *Chem. Rev.*, 2003, **103**, 4999–5024.
9. Wallington, T. J., Schneider, W. F., Sehested, J., Bilde, M., Platz, J., Nielsen, O. J. and Christensen, L. K., Atmospheric chemistry of HFE-7100 ($C_4F_9OCH_3$): reaction with OH radicals, UV spectra and kinetic data for $C_4F_9OCH_2$• and $C_4F_9OCH_2O_2$• radicals, and the atmospheric fate of $C_4F_9OCH_2O$• radicals. *J. Phys. Chem. A*, 1997, **101**, 8264–8274.
10. Mellouki, A., Teton, S. and Gras, G. Le, Kinetics of OH radical reactions with a series of ethers. *Int. J. Chem. Kinet.*, 1995, **27**, 791–805.
11. Seinfeld, J. H. and Pandis, S. N., *Atmospheric Chemistry and Physics*, John Wiley, NY, 1998.
12. Zhao, Z., Huskey, D. T., Olsen, K. J., Nicovich, J. M., McKee, M. L. and Wine, P. H., Kinetics mechanism, and thermochemistry of the gas-phase reaction of atomic chlorine with pyridine. *Phys. Chem. Chem. Phys.*, 2007, **9**, 4383–4394.
13. DeMore, W. B. *et al.*, *Chemical Kinetics and Photochemical Data for Use in Stratospheric Modeling*, JPL Publication, 97-4, 1997.
14. Wang, Y., Liu, J.-Y., Li, Z.-S., Wang, L., Wu, J.-Y. and Sun, C.-C., Theoretical studies on dynamics and thermochemistry of the reactions CHClFCHO, CHF_2CHO and $CClF_2CHO$ with the Cl atom. *Chem. Phys.*, 2006, **324**, 609–621.
15. Papadimitriou, V. C., Kambanis, K. G., Lazarou, Y. G. and Papagiannakopoulos, P., Kinetic study for the reactions of several hydrofluoroethers with chlorine atoms. *J. Phys. Chem. A*, 2004, **108**, 2666–2674.
16. Oyaro, N., Sellevag, S. R. and Nielsen, C., Atmospheric chemistry of hydrofluoroethers: reaction of a series of hydrofluoroethers with OH radicals and Cl atoms, atmospheric lifetimes, and global warming potentials. *J. Phys. Chem. A*, 2005, **109**, 337–346.
17. Dalmasso, P. R., Nieto, J. D., Taccone, R. A., Teruel, M. A. and Lane, S. I., Rate constants for reaction of Cl atoms with hydrofluoroethers. *J. Phys. Org. Chem.*, 2006, **19**, 771–775.
18. Wu, J., Liu, J., Li, Z. and Sun, C., Theoretical study of the reactions of CF_3OCHF_2 with the hydroxyl radical and the chlorine atom. *ChemPhysChem*, 2004, **5**, 1336–1344.
19. Yang, L., Liu, J.-Y., Wang, L., He, H.-Q., Wang, Y. and Li, Z.-S., Theoretical studies of the reactions $CF_3CH_2OCHF_2$ + OH/Cl and its product radicals and parent ether ($CH_3CH_2OCH_3$) with OH. *J. Comput. Chem.*, 2008, **29**, 550–561.
20. Jia, X., Liu, Y., Sun, J., Sun, H., Su, Z., Pan, X. and Wang, R., Theoretical investigation of the reactions of $CF_3CHFOCF_3$ with the OH radical and Cl atom. *J. Phys. Chem. A*, 2010, **114**, 417–424.
21. Blowers, P., Tetrault, K. F. and Trujillo-Morehead, V., Global warming potential predictions for hydrofluoroethers with two carbon atoms. *Theor. Chem. Acc.*, 2008, **119**, 369–381.
22. Kambanis, K. G., Lazarou, Y. G. and Papagiannakopoulos, P., Kinetic study for the reactions of chlorine atoms with a series of hydrofluoroethers. *J. Phys. Chem. A*, 1998, **102**, 8620–8625.
23. Sander, S. P. *et al.*, Chemical kinetics and photochemical data for use in atmospheric studies: Evaluation number 15. JPL, National Aeronautics and Space Administration, Pasadena, CA, 2006.
24. Wallington, T. J., Hurley, M. D., Fedotov, V., Morrell, C. and Hancock, G., Atmospheric chemistry of $CF_3CH_2OCHF_2$ and $CF_3CHClOCHF_2$: Kinetics and mechanisms of reaction with Cl atoms and OH radicals and atmospheric fate of $CF_3C(O•)HOCF_2$ and $CF_3C(O•)ClOCHF_2$ radicals. *J. Phys. Chem. A*, 2002, **106**, 8391–8398.
25. Tauzon, E. C., Tropospheric degradation products of novel hydrofluoropolyethers. *Environ. Sci. Technol.*, 1997, **31**, 1817–1821.
26. Andersen, M. P. S., Hurley, M. D., Andersen, V. F., Nielsen, O. J. and Wallington, T. J., CHF_2OCHF_2(HFE-134): IR spectrum and kinetics and products of the chlorine-atom-initiated oxidation. *J. Phys. Chem. A*, 2010, **114**, 4963–4967.
27. Zhao, Y. and Truhlar, D. G., Hybrid meta density functional theory methods for thermochemistry thermochemical kinetics, and noncovalent interactions: the MPW1B95 and MPWB1K models and comparative assessments for hydrogen bonding and van der Waals interactions. *J. Phys. Chem. A*, 2004, **108**, 6908–6918.
28. Zhao, Y., Schultz, N. E. and Truhlar, D. G., Design of density functionals by combining the method of constraint satisfaction with parametrization for thermochemistry, thermochemical kinetics, and noncovalent interactions. *J. Chem. Theor. Comput.*, 2006, **2**, 364–382.
29. Devi, Kh. J. and Chandra, A. K., Theoretical studies on the kinetics and thermochemistry of the gas-phase addition and H-abstraction reactions of 4-picoline with OH radical. *Chem. Phys. Lett.*, 2009, **480**, 161–167.
30. Devi, Kh. J. and Chandra, A. K., Kinetics and thermochemistry of the gas-phase reactions of 4-ethylpyridine with OH radical: A DFT study. *Comput. Theor. Chem.*, 2011, **965**, 268–274.
31. Curtiss, L. A., Raghavachari, K. and Pople, J. A., Gaussian-2 theory using reduced Moller–Plesset orders. *J. Chem. Phys.*, 1993, **98**, 1293–1298; E_{G2MP2} = E(QCISD(T)/6-311G(d,p)) + [E(MP2/6-311 + G(3df,2p)–E(MP2/6-311G(d,p)] + HLC + E(ZPE), where HLC is the empirical high-level correlation correction.
32. Devi, Kh. J. and Chandra, A. K., Theoretical investigation of the gas-phase reactions of $(CF_3)_2CHOCH_3$ with OH radical. *Chem. Phys. Lett.*, 2011, **502**, 23–28.
33. Frisch, M. J. *et al.*, GAUSSIAN 03, Revision C.01, Gaussian Inc., Wallingford, CT, 2004.
34. Laidler, K. J., *Chemical Kinetics*, Pearson Education, Delhi, 2004, 3rd edn.
35. Johnston, H. S. and Heicklen, J., Tunnelling corrections for unsymmetrical EckartT potential energy barriers. *J. Phys. Chem.*, 1962, **66**, 532–533.
36. Tunnelling correction factor $\Gamma(T)$ was estimated using our own program. Numerical integration was carried out using trapezoidal method with a stepsize of 2.5×10^{-5} and using 8×10^6 steps.
37. Truhlar, D. G., Simple approximation for the vibrational partition function of hindered internal rotation. *J. Comput. Chem.*, 1991, **12**, 266–270.
38. Ayala, P. Y. and Schlegel, H. B., Identification and treatment of internal rotation in normal mode vibrational analysis. *J. Chem. Phys.*, 1998, **108**, 2314–2325.
39. Chase Jr, M. W., Davies, C. A., Downey Jr, J. R., Frurip, D. J., McDonald, R. A. and Syverud, A. N., *JANAF Thermochemical Tables*, *J. Phys. Chem. Ref. Data* 14, 1985, Suppl. 1, 3rd edn.
40. Hammond, G. S., A correlation of reaction rates. *J. Am. Chem. Soc.*, 1955, **77**, 334–338.
41. Lide, D. R. (ed.), *CRC Handbook of Chemistry and Physics*, CRC Press, NY, 2008–2009, 89th edn.
42. Chandra, A. K. and Uchimaru, T., The C–H bond dissociation enthalpies of haloethers and its correlation with the activation energies for hydrogen abstraction by OH radical: A DFT study. *Chem. Phys. Lett.*, 2001, **334**, 200–206.
43. McQuarrie, D. A., *Statistical Mechanics*, VIVA Books Pvt Ltd, New Delhi, 2003.
44. Kurylo, M. J. and Orkin, V. L., Determination of atmospheric lifetimes via the measurement of OH radical kinetics. *Chem. Rev.*, 2003, **103**, 5049–5076.
45. Spicer, C. W., Chapman, E. G., Finlayson-Pitts, B. J., Plastridge, R. A., Hubbe, J. M., Fast, J. D. and Berkowitz, C. M., Unexpectedly high concentration of molecular chlorine in coastal air. *Nature*, 1998, **394**, 353–355.

ACKNOWLEDGEMENTS. A.K.C. thanks CSIR, New Delhi for providing financial assistance through a project (No. 01(2494)/11/EMR-II). Kh.J.D. thanks NEHU, Shillong for a research fellowship.